NGL-05-002-130

DETECTION OF [Ni II] λ7378 IN SIX SEYFERT GALAXIES

J. P. Halpern
Columbia Astrophysics Laboratory, Columbia University

J.B. Oke
Palomar Observatory, California Institute of Technology

Received:

Abstract

We detect a line due to [Ni II] λ7378 in the Seyfert galaxies NGC 1068, 2110, 3227, 4151, 5506, and Arp 102 B. The average Ni abundance is about 2 times solar, which is 5 times less than in the filaments of the Crab Nebula. This argues for nucleosynthetic processing in the latter. The [Ni II] line is spatially resolved in NGC 1068, and shows at least a factor of 4 enhancement in the Ni abundance away from the nucleus. The off-nuclear abundance of Ni in NGC 1068 approaches that of the Crab, which strongly suggests that type II supernovae enriched the off-nuclear gas clouds.

Subject headings: Galaxies: Seyfert - Line Identifications - Abundances

I. Introduction

The detection of nickel in Seyfert galaxies irst reported by Grandi (1978), who found a line corresponding to [Ni II] λ7377.8 in NGC 4151 and NGC 1068. This forbidden line arises from the ground state of Ni^{+}, which has an ionization potential of 18.18 eV, and should be associated with other low-ionization species such as [S II] and [O I]. Based on the absence of another member of the same multiplet, [Ni II] λ7411.6, Grandi concluded that [Ni II] λ7378 is not be the sole contributor to the observed line. He suggested the presence of [Fe II] λ7388.2. The λ7378 line is strong in several supernova remnants, including IC 443 (Fesen and Krishner 1980) and the Crab Nebula (Fesen and Kirshner 1982; Dennefeld and Péquignot 1983; Henry, MacAlpine and Kirshner 1984). Nussbaumer and Storey (1982) calculated transition probabilities and collision strengths for the relevant multiplets of [Ni II], and showed that the intensity ratio of λ7412/λ7378 is expected to be less than 0.1 under conditions of density and temperature which prevail in the Crab filaments and Seyfert narrow-line regions. Thus, the absence of λ7412 is not a reason to doubt the identification of the line at 7378 Å with [Ni II].

In this letter, we confirm the existence of [Ni II] λ7378 in NGC 1068 and NGC 4151, and report its detection in four additional Seyfert galaxies, NGC 2110, NGC 3227, NGC 5506, and Arp 102 B. We estimate the abundance of nickel following the method used by Henry (1984) for the Crab Nebula filaments. Henry found a wide range of nickel abundances at different positions in the Crab, with the average being a factor of 10 above the solar value. This was especially surprising in view of the fact

that the iron abundance derived using [Fe II] λ8617 was substantially below solar, so that [Ni/Fe] in the Crab filaments has an average value of 43 times the solar level. A similar conclusion was reached by Dennefeld and Péguignot (1983) for the Crab.

The importance of the Seyfert galaxies is in providing a benchmark value of [Ni/Fe] from material which is supposedly unprocessed. It is fortunate that the power-law photon spectrum and ionization parameter are remarkably similar in Seyfert galaxies and the Crab Nebula. Therefore, differences in the structure of the photoionized nebulae are largely eliminated as a consideration in the relative abundance analysis.

II. Observations

Many of the spectra were obtained on partly cloudy nights using the red camera (TI CCD) of the Double Spectrograph (Oke and Gunn 1982) on the Hale 5 m telescope. The dispersion was 6 Å per pixel, with a resolution of 12 Å. Comparison spectra of helium and argon permitted wavelength fits with rms deviation of 0.3 Å. The single exception is the spectrum of Arp 102 B, which was observed with ~ 2 Å resolution using the same instrument under photometric conditions.

Three complicating factors affect the detection and measurement of [Ni II] λ7378 in Seyfert galaxies. First, the head of the atmospheric A band at 7590 Å effectively limits the search to galaxies with $v < 8000$ km s^{-1}. The highest velocity object in our sample is Arp 102 B, with $v = 7310$ km s^{-1}. Second, the weak [Ni II] line is detectable only in Seyfert galaxies with strong lines of other low-ionization species such as [S II]

and [O I]. Unfortunately, these tend also to be objects in which the stellar contribution to the continuum is substantial, making the measurement of weak lines difficult. Nevertheless, the [Ni II] line is well detected in all of our objects. Third, forbidden lines of different species often have velocities which differ systematically as a function of ionization potential by as much as 300 km s^{-1}. This makes the expected position of the [Ni II] possibily uncertain by ~ 7 Å.

In order to minimize the effect of possible systematic errors in wavelength calibration, we determined a redshift using the nearby line of [A III] 7135.8 wherever possible. In the case of Arp 102 B, the resolved [S II] lines were used, and for NGC 2110, the redshift was derived from the [O II] λλ7319,7330 blend at an assumed mean wavelength of 7324 Å. The adopted redshifts and derived rest wavelengths of the supposed [Ni II] line are listed in Table 1. The wavelengths are all within 1.5 Å of the position of [Ni II] or within 0.6 Å if NGC 1068 is excluded. A check on the validity of the redshift determination using [O II] λ7319, 7330 and other low ionization lines confirms that the identification of [Ni II] is secure in every case. In particular, there is no evidence for the presence of [Fe II] λ7388. Confirming spectra were obtained during independent observing runs for all objects except NGC 5506 [but see Morris and Ward (1985)]. Following the example of Henry, we measured the flux of [Ni II] relative to [S II] λλ6717,6731. The quantity $R_{Ni} \equiv 100 \times I(7378)/I(6717+31)$, uncorrected for reddening, is also listed in Table 1.

III. Notes on Individual Galaxies

a) NGC 1068

This is the only galaxy in which the [Ni II] emission is spatially resolved. It is not clear whether the line is detected in the nucleus. The long-slit spectrum taken at position angle 37° shows that the strength of [Ni II] relative to [S II] or [O II] rises as a function of distance from the nucleus (Fig. 1) as far as the signal-to-noise ratio permits it to be followed (up to ~5"). The off-nuclear spectrum between 2".6 and 4".4 is redshifted by ~ 600 km s^{-1} from the nuclear spectrum, and so corresponds to cloud 1 of Walker (1968). Apparently this cloud has a much larger nickel abundance than the nuclear continuum source. This off-nuclear region is also coincident with the northeast radio lobe of van der Hulst, Hummel, and Dickey (1982), and Wilson and Ulvestad (1983), which extends to 5".6 from the nucleus at position angle 33°. NGC 1068 has the strongest [Ni II] line of all our objects.

b) NGC 2110

This X-ray-discovered active elliptical galaxy has very strong [OI] and [S II] lines, making it a relative of the Liners (Halpern and Steiner 1983). A substantial stellar continuum is responsible for the broad TiO absorption feature around 7200 Å.

c) NGC 3227

He I λ7065 emission is broad, and superposed on TiO absorption. The stellar continuum is strong.

d) NGC 4151

The upper spectrum (Fig. 2) is a longer exposure (in which Hα was saturated) taken to bring out faint features.

e) NGC 5506

NGC 5506 is another X-ray-discovered Seyfert galaxy with prominent [S II] lines. The [Ni II] line is apparent in the spectrum of Morris and Ward (1985), although not mentioned by them.

f) Arp 102 B

This elliptical galaxy has a peculiar broad Hα profile resembling that of 3C390.3. It is a radio and an X-ray source (Biermann et al. 1981). The strong low-ionization lines put it in the Liner category (Stauffer, Schild and Keel 1983). The inset (Fig. 3) shows an expanded view of the region around [Ni II]. Emission of [Ca II] λ7291.5 is apparent, and so [Ca II] λ7323.9 probably makes a significant contribution to [O II] λλ7319,7330. [Ca II] λ7291 is also evident as a blue wing on the [O II] line in NGC 2110, NGC 5506, and possibly NGC 1068. The continuum is predominantly stellar. The overall spectrum of Arp 102 B will be discussed in detail in a future paper.

IV. Nickel Abundance and [Ni/Fe] Ratio

Henry (1984) determined the abundance of Ni relative to S in the Crab Nebula filaments using the data of Henry, MacAlpine and Kirshner (1984). The ratio R_{Ni} = 100 × I[Ni II]/I[S II] in the Crab ranges between 5 and

42, with a mean of 16. The derived [Ni/S] abundance ratio is approximately 0.67 R_{Ni}, or on average 10 times the solar value. The [Fe/S] ratio was measured in an analogous manner using [Fe II] λ8617. In the Crab, the ratio $R_{Fe} = 100 \times I[Fe\ II]/I[S\ II]$ has an average value of 7.5, corresponding to [Fe/S] of 0.37 times the solar value. Equivalently, the average of [Ni/Fe] was found to be 43 times the solar value. Three possible explanations offered by Henry for these results are: (1) production and subsequent ejection of neutron rich species (i.e. Ni) from the core of the massive progenitor of a type II supernova; (2) preferential depletion of Fe onto grains; and (3) inadequacies in the atomic data, or physical processes not taken into account.

We also measured the flux of [Fe II] 8717 in the 5 Seyfert galaxies for which the spectra covered this region. The results are listed in Table 1. The flux of this line is quite uncertain because it is superposed on the absorption lines of the Ca II infrared triplet. The average of the ratios R_{Ni} and R_{Fe} are both about 3 in the Seyfert galaxies (neglecting for the moment the unusual case of NGC 1068). The detection of [Ni II] λ7378 in Seyfert galaxies provides a valuable discriminator between Henry's three hypotheses. Since the physical conditions in the [S II] emitting regions of Seyfert galaxies and the Crab filaments are very similar ($T \sim 10^4$ K, $n_e \sim 10^3$ cm^{-3}, $f_\nu \propto \nu^{-1.1}$), possibilities (2) and (3) cannot account for the differences in apparent Ni abundance between the Crab and the Seyfert galaxies. Therefore, the Ni abundance must really be about 5 times higher in the Crab than in the Seyfert galaxies as a result of nucleosynthetic processes. The Fe abundance is probably also higher by about a factor of 2 in the Crab than in the Seyfert galaxies.

Apparently, the [Ni/S] ratio in the Seyfert galaxies is only a factor of 2 above solar, while the [Ni/Fe] ratio is about 13 times solar. These remaining discrepancies may be in part due to preferential depletion of Fe onto grains, or poorly understood atomic processes, but it seems clear that the major part of the difference in [Ni II] line strength between the Crab and the Seyfert galaxies is due to a real abundance enhancement in the Crab. The recent detection of a density gradient in the forbidden-line regions of some Seyfert galaxies and Liners (Filippenko and Halpern 1984; Filippenko 1985) cannot account for the difference in [Ni II] strength between the Crab and the Seyferts. The higher critical density of [Ni II] ($n_e \sim 10^7$ cm^{-3}, Nussbaumer and Storey 1982) could only serve to <u>increase</u> its strength relative to [S II].

Under this interpretation, the large Ni and Fe abundances in the off-nuclear spectrum of NGC 1068 approach the values seen in the Crab filaments. Condon *et al.* (1982) and van der Hulst, Hummel, and Dickey (1982) have argued that supernovae are responsible for the radio emission in NGC 1068, whereas Wilson and Ulvestad (1983) favor a jet model. The evidence for starburst activity in NGC 1068 was recently reviewed by Balick and Heckman (1985). The [Ni II] line behavior strongly argues that the off-nuclear cloud is made of material which was recently processed through type II supernovae, and that more recent star formation has taken place outside the central continuum source than near it.

V. Conclusions

The detection of [Ni II] λ7378 is favored in Seyfert galaxies with strong lines of low-ionization species such as [S II] and [O I]. However, there is no indication that the relative abundance of Ni in these objects is unusual among Seyfert galaxies. A comparison with the spectra of filaments in the Crab Nebula shows that the Ni abundance of the latter is enhanced by at least a factor of 5 as a result of nucleosynthetic processes. A gradient in the [Ni II] and [Fe II] lines in NGC 1068 strongly suggests that type II supernovae are responsible for enriching the off-nuclear gas clouds.

This work was supported by NASA grant NGL 05-002-134 to J.B.O. and by NASA contract NAG 8-497 to the Columbia Astrophysics Laboratory. This article is Columbia Astrophysics Laboratory Contribution Number 295.

Table 1

[Ni II] and [Fe II] Emission-Line Data

Galaxy	z	[Ni II] λ7377.8 measured wavelength	R_{Ni}	R_{Fe}
NGC 1068 (nucl.)	0.00338	--	< 2.	< 2.
NGC 1068 (off nucl.)	0.00530	7379.3	7.9	9.2
NGC 2110	0.00773	7377.6	3.0	4.1
NGC 3227	0.00317	7377.4	3.1	< 2.
NGC 4151	0.00310	7377.9	1.9	2.6:
NGC 5506	0.00683	7378.4	1.5	3.7
Arp 102 B	0.02439	7377.2	5.4	--
Crab (mean)[1]			16.	7.5

Notes: R_{Ni} = 100 × I [Ni II] 7378 / I [S II] 6717+31

R_{Fe} = 100 × I [Fe II] 8617 / I [S II] 6717+31

[1] Crab data from Henry, MacAlpine, and Kirshner (1984)

References

Balick, B. and Heckman, T. 1985, A.J., 90, 197.

Biermann, P. Kronberg, P.P., Preuss, E. Schilizzi, R.T., and Shaffer, D.B. 1981, Ap.J. (Letters), 250, L49.

Condon, J.J., Condon, M.A., Gisler, G., and Puschell, J.J. 1982, Ap.J., 252, 102.

Dennefeld, M. and Péquignot, D. 1983, Astr. Ap., 127, 42.

Fesen, R.A. and Kirshner, R.P. 1980, Ap.J., 242, 1023.

Fesen, R.A. and Kirshner, R.P. 1982, Ap.J., 258, 1.

Filippenko, A.V. 1985, Ap.J., 289, 475.

Filippenko, A.V. and Halpern, J.P. 1984, Ap.J., 285, 458.

Grandi, S.A. 1978, Ap.J., 221, 501.

Halpern, J.P. and Steiner, J.E. 1983, Ap.J. (Letters), 269, L37.

Henry, R.B.C. 1984, Ap.J., 281, 644.

Henry, R.B.C., MacAlpine, G.M., and Kirshner, R.P. 1984, Ap.J., 278, 619.

Morris, S.L. and Ward, M.J. 1985, M.N.R.A.S., submitted.

Nussbaumer, H. and Storey, P.J. 1982, Astr. Ap., 110, 295.

Oke, J.B. and Gunn, J.E. 1982, Pub. A.S.P., 94, 586.

Stauffer, J., Schild, R., and Keel, W. 1983, Ap.J., 270, 465.

van der Hulst, J.M., Hummel, E., and Dickey, J.M. 1982, Ap.J. (Letters), 261, L59.

Walker, M.F. 1968, Ap.J., 151, 71.

Wilson, A.S. and Ulvestad, J.S. 1983, Ap.J., 275, 8.

Figure Captions

Figure 1 (a) Spatially resolved spectra of NGC 1068 along position angle 37°. Observed wavelength is plotted. Hα and [S II] are saturated in the nucleus. The relative strength of the [Ni II] and [Fe II] lines is greater off the nucleus.

(b) The off-nuclear spectrum of NGC 1068 corresponding to cloud 1 of Walker (1968). This is the same as the lower trace in (a), except that rest wavelength is plotted.

Figure 2 Spectra of NGC 2110, 3227, 4151, and 5506 showing the [Ni II] lines. Note the contribution of [Ca II] λ7291 in NGC 2110 and NGC 5506. Rest wavelength is plotted.

Figure 3 Spectrum of Arp 102 B with ~2 Å resolution. The region around the atmospheric A-band has been removed. The inset shows a blowup of the region around [Ni II]. Rest wavelength is plotted.

Authors' Addresses

J.P. Halpern

Columbia Astrophysics Laboratory

Columbia University

538 W. 120th Street

New York, New York 10027

J.B. Oke

Astronomy Department, 105-24

California Institute of Technology

Pasadena, California 91125

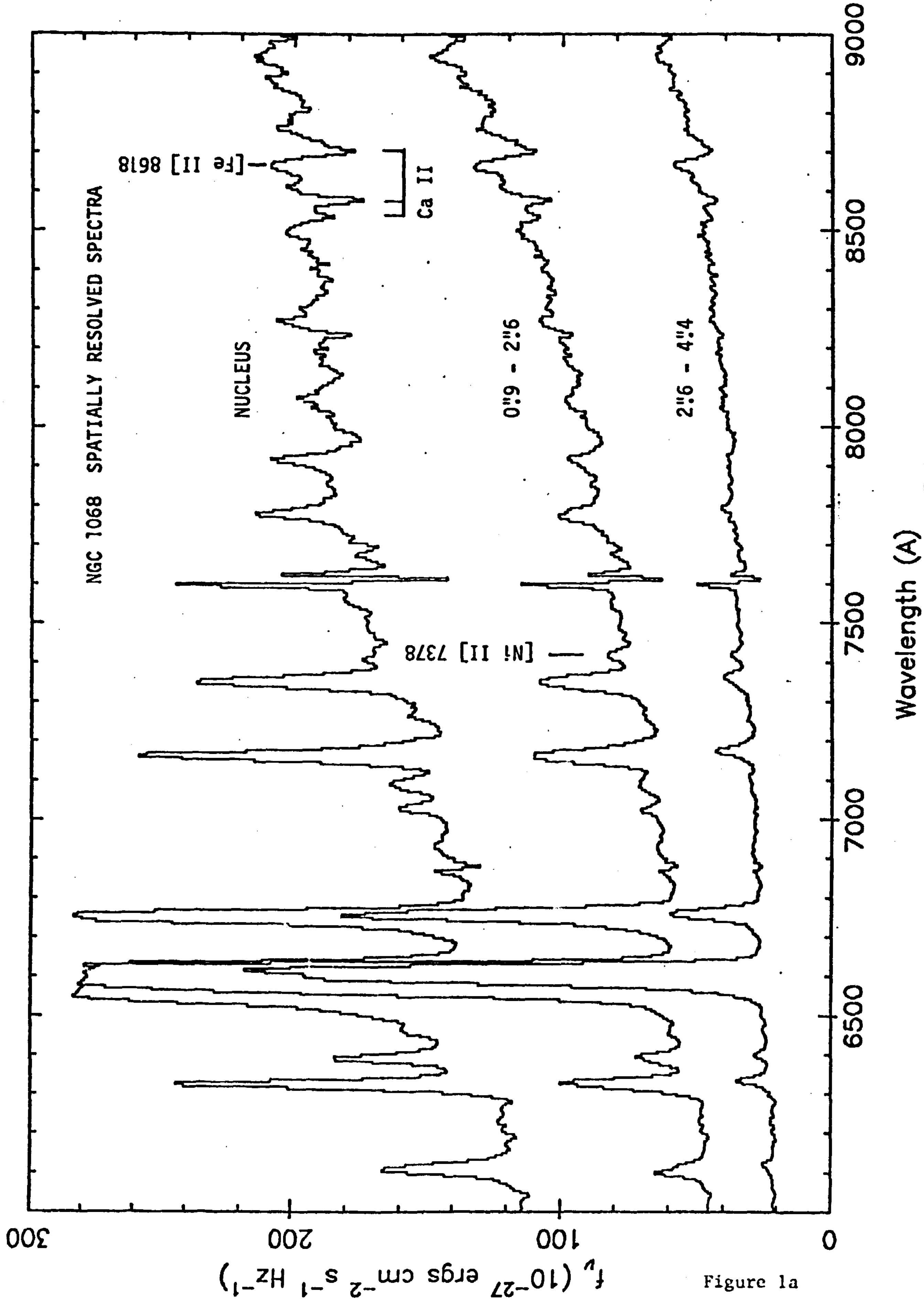
NGC 1068 SPATIALLY RESOLVED SPECTRA
NUCLEUS
0"9 - 2"6
2"6 - 4"4
[Fe II] 8618
Ca II
[Ni II] 7378
Wavelength (A)
f_ν (10^{-27} ergs cm^{-2} s^{-1} Hz^{-1})
0
100
200
300
6500
7000
7500
8000
8500
9000

Figure 1a

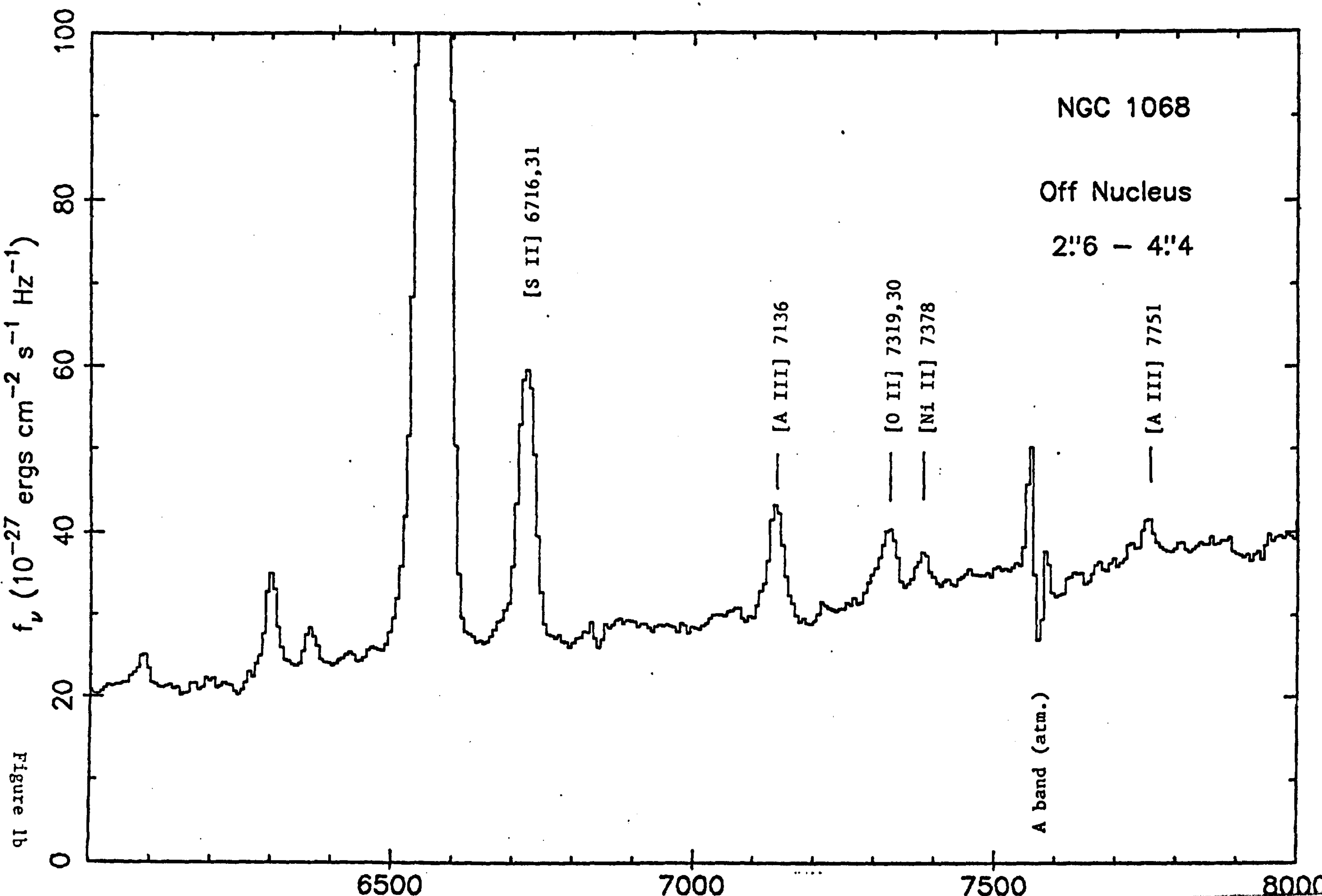
NGC 1068
Off Nucleus
2"6 – 4"4
[S II] 6716,31
[A III] 7136
[O II] 7319,30
[Ni II] 7378
[A III] 7751
A band (atm.)
f_ν (10^{-27} ergs cm^{-2} s^{-1} Hz^{-1})
100
80
60
40
20
0
6500
7000
7500
8000

Figure 1b

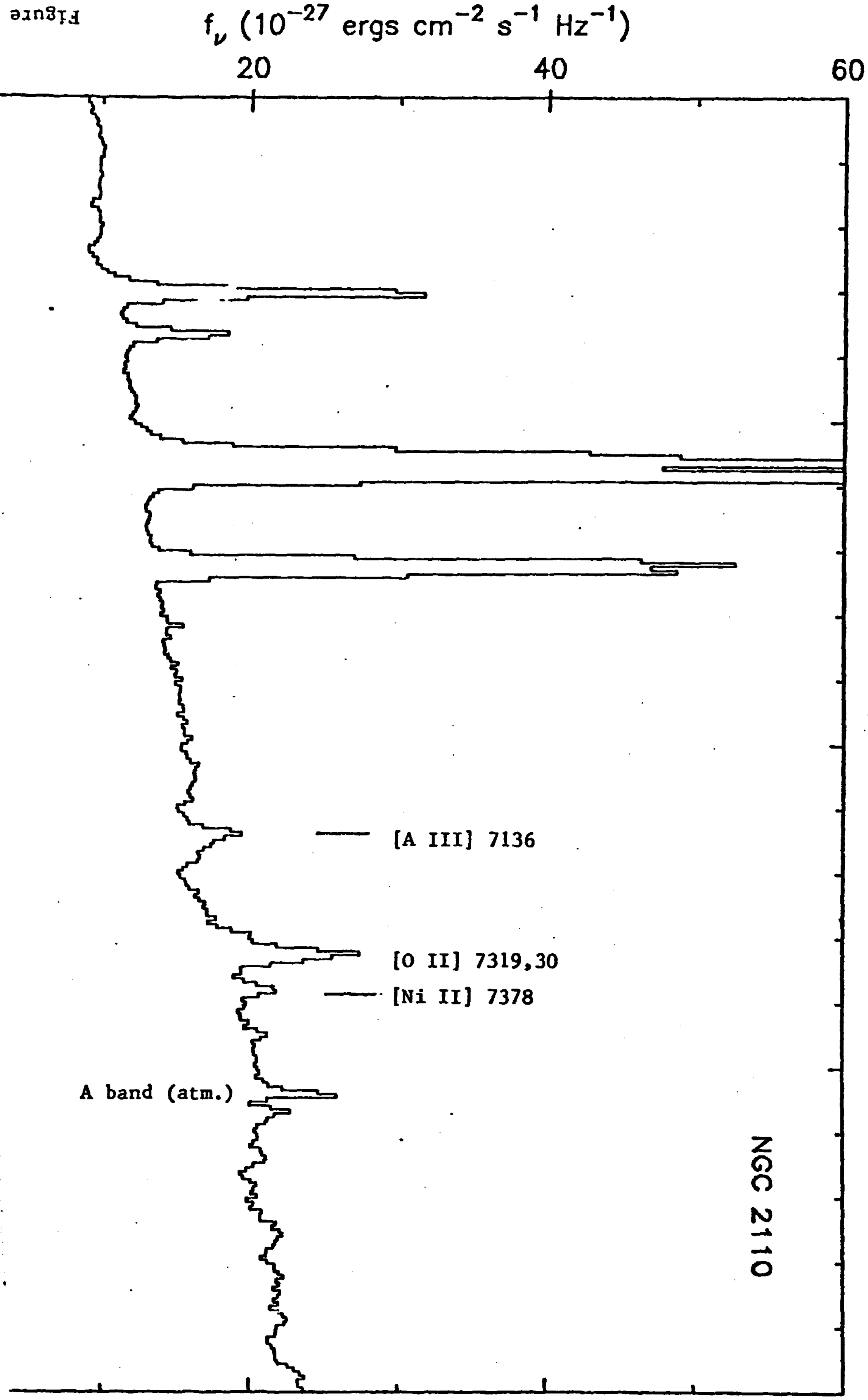
f_ν (10^{-27} ergs cm^{-2} s^{-1} Hz^{-1})
20
40
60
NGC 2110
[A III] 7136
[O II] 7319,30
[Ni II] 7378
A band (atm.)

Figure 2a

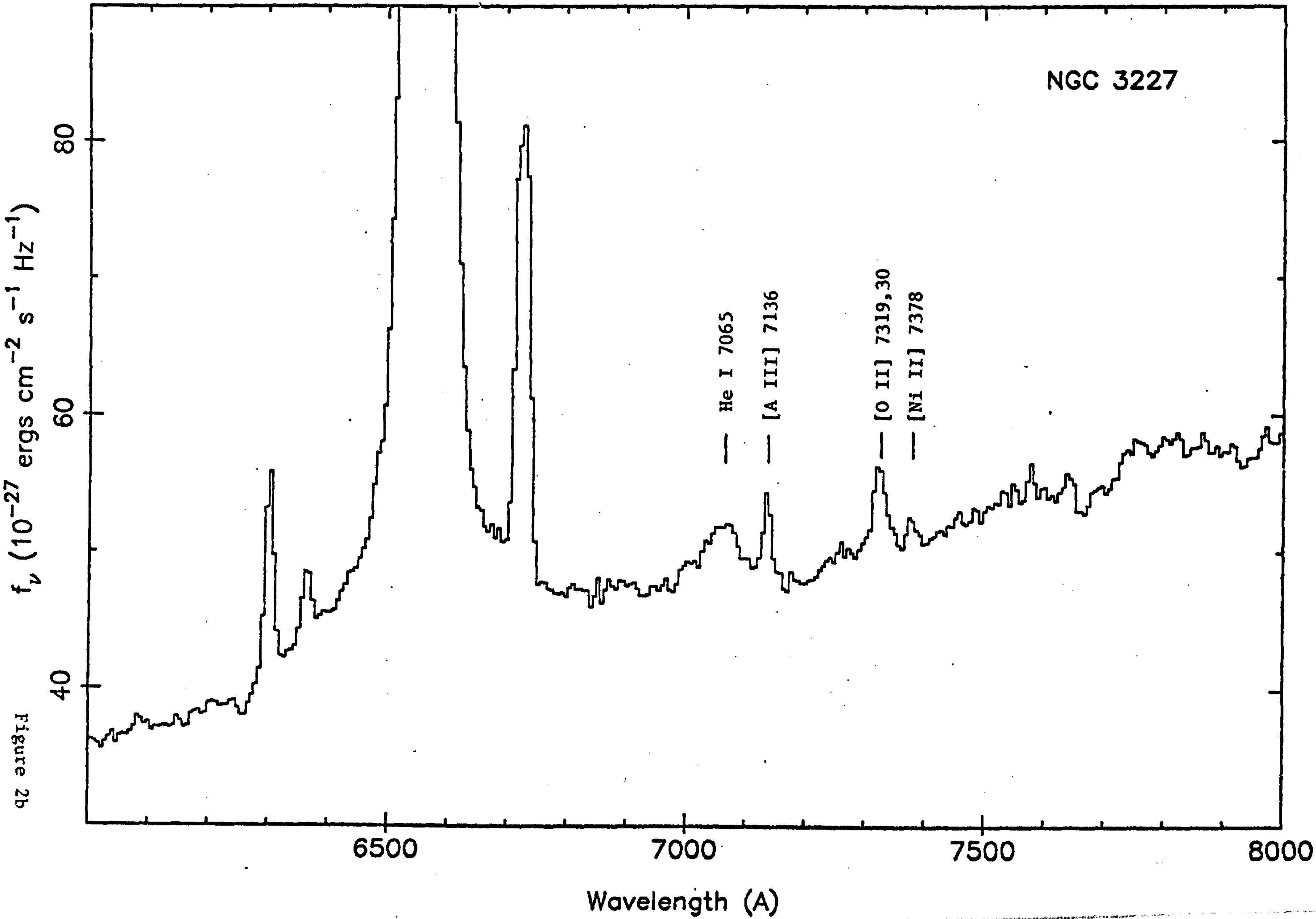
NGC 3227
He I 7065
[A III] 7136
[O II] 7319,30
[Ni II] 7378
80
60
40
6500
7000
7500
8000
f_ν (10^{-27} ergs cm^{-2} s^{-1} Hz^{-1})
Wavelength (A)

Figure 2b

19

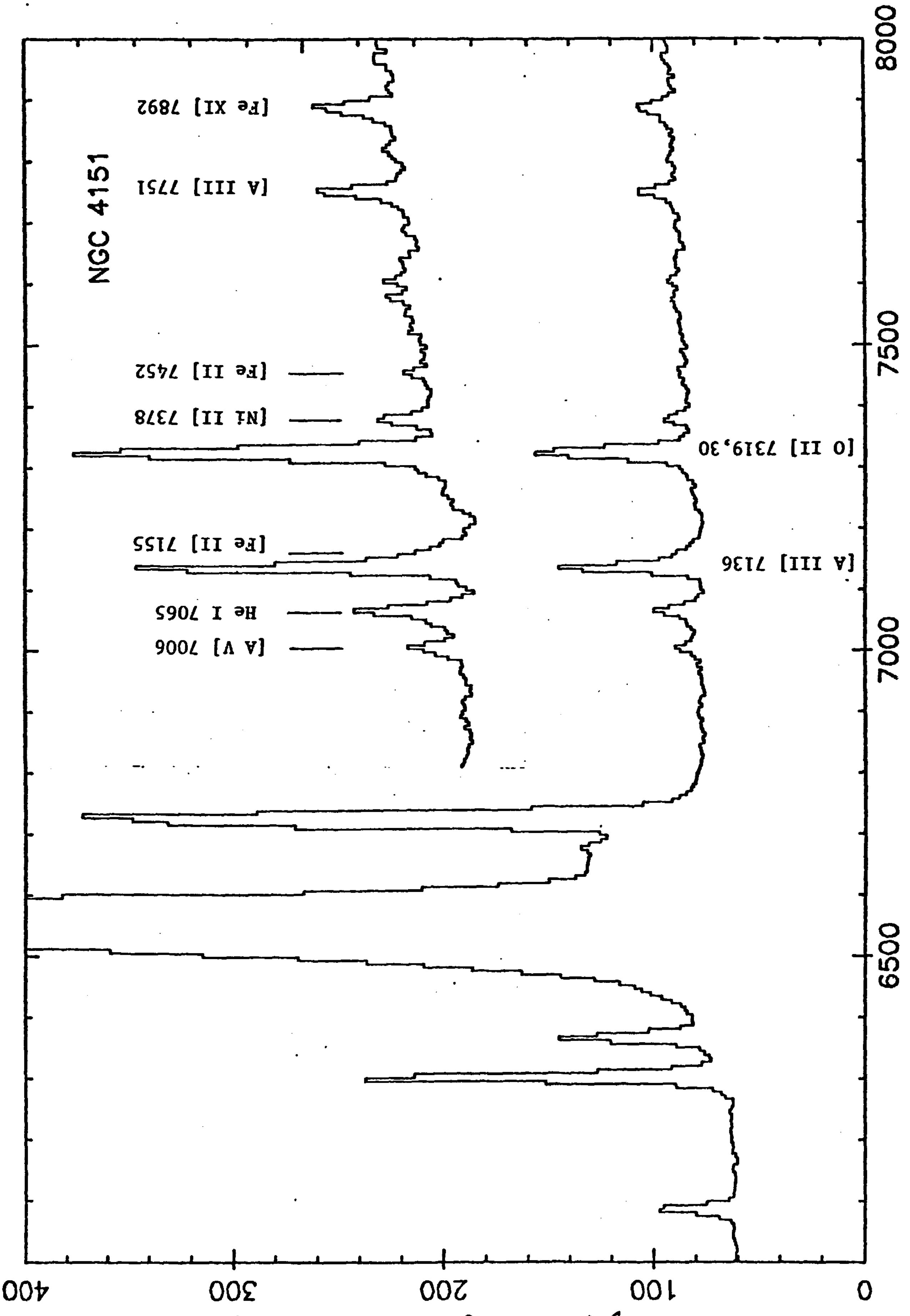

NGC 4151
[Fe XI] 7892
[A III] 7751
[Fe II] 7452
[Ni II] 7378
[O II] 7319,30
[Fe II] 7155
[A III] 7136
He I 7065
[A V] 7006
8000
7500
7000
6500
Wavelength (Å)
400
300
200
100
0
f_ν (10^{-27} ergs cm^{-2} s^{-1} Hz^{-1})

Figure 2c

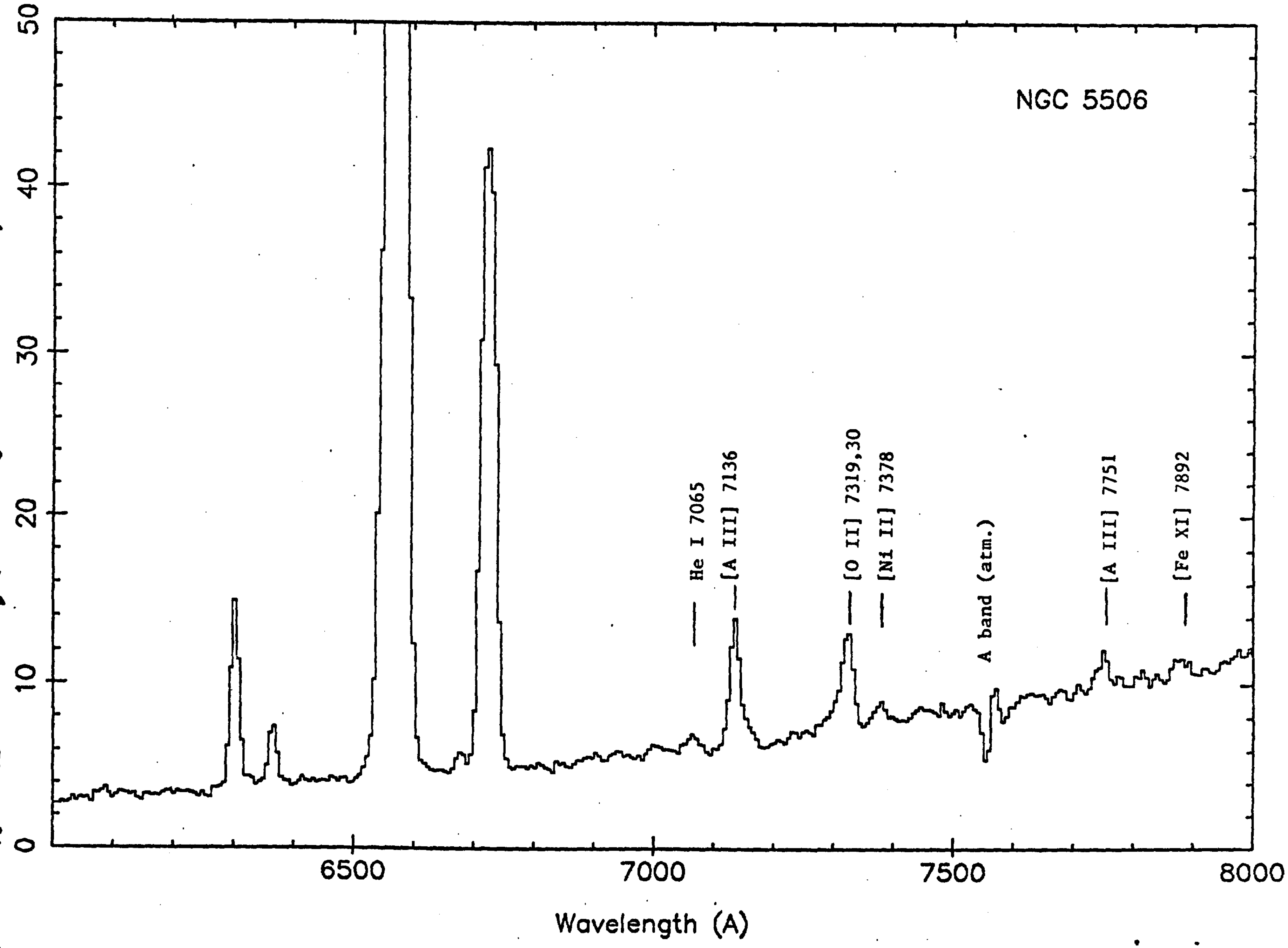
NGC 5506
f_ν (10^{-27} ergs cm^{-2} s^{-1} Hz^{-1})
Wavelength (A)
0
10
20
30
40
50
6500
7000
7500
8000
He I 7065
[A III] 7136
[O II] 7319,30
[Ni II] 7378
A band (atm.)
[A III] 7751
[Fe XI] 7892

Figure 2d

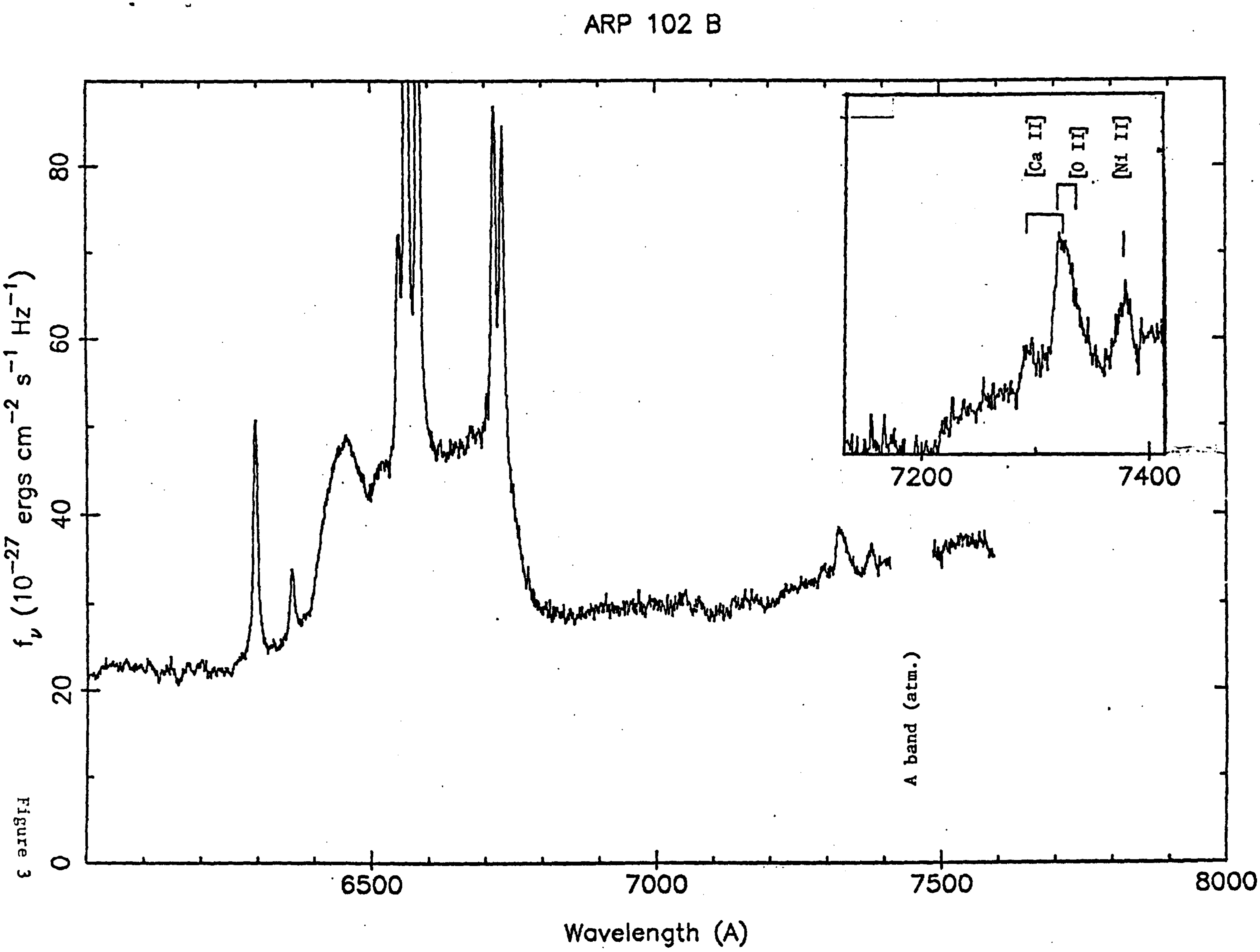
ARP 102 B
[Ca II]
[O II]
[Ni II]
7200
7400
A band (atm.)
f_ν (10^{-27} ergs cm^{-2} s^{-1} Hz^{-1})
0
20
40
60
80
6500
7000
7500
8000
Wavelength (A)

Figure 3

20